

PAPER

Modeling spectral correlations of photon-pairs generated in liquid-filled photonic crystal fibers

To cite this article: Lorena Velázquez-Ibarra *et al* 2020 *J. Opt.* **22** 075203

View the [article online](#) for updates and enhancements.




IOP | ebooks™

Bringing together innovative digital publishing with leading authors from the global scientific community.

Start exploring the collection—download the first chapter of every title for free.

Modeling spectral correlations of photon-pairs generated in liquid-filled photonic crystal fibers

Lorena Velázquez-Ibarra¹ , Antonio Díez² , Enrique Silvestre³ , Miguel V Andrés² 
and J L Lucio^{1,4}

¹ Departamento de Física, Universidad de Guanajuato, Loma del Bosque 103, 37150, Mexico

² Departamento de Física Aplicada y Electromagnetismo-ICMUV, Universidad de Valencia, Dr Moliner 50, 46100, Spain

³ Departamento de Óptica-ICMUV, Universidad de Valencia, Dr Moliner 50, 46100, Spain

E-mail: lorenav@fisica.ugto.mx

Received 25 April 2020

Accepted for publication 29 May 2020

Published 25 June 2020



CrossMark

Abstract

The generation of photon-pairs with controllable spectral correlations is crucial in quantum photonics. Here we present the design of a photonic crystal fiber to generate widely-spaced four-wave mixing bands with spectral correlations that can be tuned through the thermo-optic effect after being infiltrated with heavy water. We present a theoretical study of the purity of the signal and idler photons generated as a function of temperature, pump spectral linewidth and the length of the fiber.

Keywords: non-linear optics, photon sources, microstructured optical fibers, spectral correlations

(Some figures may appear in colour only in the online journal)

1. Introduction

Photons are one of the most useful carriers of quantum information and the building blocks in quantum optics applications. Some of these applications rely on photon pairs in a maximally entangled state, such as quantum optical coherence tomography [1], quantum teleportation [2] or quantum cryptography with entanglement-based quantum key distribution (QKD) protocols [3, 4]. However, there are also applications, such as some QKD protocols [5, 6], where entanglement needs to be avoided and pure single-photon states should be used. It has been shown that photon pairs in factorable states generated by spontaneous four wave mixing (FWM) in optical fibers can be used as a source of high-purity single photons [7, 8]. Hence, photon-pair sources capable of generating and controlling the desired states are a fundamental element of many quantum optics experiments.

It is essential that these sources generate photons not only in the correct state for the needed application, but also at

wavelengths for optimal detection with the currently available single-photon detectors (SPD). The development and implementation of light sources based on non-linear optics with engineered generation of photon pairs has greatly benefited from photonic crystal fibers (PCF) [9–12]. PCF can be fabricated with highly tailored dispersion profiles, allowing for a precise control in the generation of non-linear effects such as four-wave mixing. In order to produce heralded pure single photons in single-mode fibers, it is necessary to remove entanglement in polarization and frequency.

The strong spectral correlations shown, in general, by photon-pairs generated by FWM in PCF are not easy to remove, but it can be achieved by tailoring the PCF dispersion profile to obtain group-velocity matching (GVM) [10] in addition to phase-matching (PM). The typical behavior of the dispersion curve of a silica PCF, in the 1–2 μm region, is a growing function with wavelength, with one zero dispersion wavelength (ZDW). Stronger variations in the dispersion profile open up the possibility of engineering the matching conditions; for this reason, fibers with two ZDW are suitable candidates for GVM. A limitation of this scheme, however, is that once a fiber with the selected design is fabricated, its

⁴ Present address: Institut für Angewandte Physik, Wegelerstr. 8, 53115 Bonn, Germany

dispersion profile is fixed and the FWM process can then only be modified through either the pump parameters [13, 14] or the fiber length [15, 16].

The ability to actively tune the dispersion properties of the fiber is desirable in order to have a photon-pair source with controllable spectral correlations without the need of (bulky and expensive) tunable lasers or of modifying fundamental elements of the source, such as the fiber itself. Some attempts have been reported in this direction. The effect that temperature variations and longitudinal stress applied to a PCF have on the spectral correlations of FWM photon-pairs was investigated in [17], where wavelength tuning is achieved while leaving the spectral correlations unaffected. The spectral correlations of modulation instability (MI) generated photon pairs in gas-filled hollow-core PCF are investigated as a function of gas pressure, fiber length and pump chirp in [18]. In [16] gas-filled hollow-core PCFs are studied as well, but in this case the spectral correlations of FWM generated photon-pairs are investigated; the correlations are adjusted with the length of the fiber while wavelength tuning is achieved through pressure changes in the PCF; fine tuning of the spectral correlations with gas pressure is also predicted through simulations.

In this paper, we propose a design for a liquid-filled solid-core PCF that, in contrast with previous approaches, allows broad dynamic shaping of the photon-pair spectral correlations with temperature. This dynamic control is external in the sense that neither the fiber length nor the pump parameters need to be modified to tune the correlations. The fiber is designed to generate FWM bands spectrally far away from Raman scattering, which is a known source of noise in fiber-based photon-pair sources [19]. We chose heavy water as the filling liquid because it has a refractive index lower than silica, a large thermo-optic coefficient (almost one order of magnitude larger than silica), and low absorption at the wavelengths of interest [20]. The large thermo-optic coefficient of heavy water is exploited as a means to dynamically induce significant changes in the dispersion profile of the liquid-filled PCF and, hence, in the FWM process [21] and spectral correlations. Although liquid-filled PCFs have been investigated in the past for thermal tuning of the dispersion [21, 22], that work was focused in the normal dispersion regime and no attention was paid to the spectral correlations. Now, we demonstrate that thermal tuning of liquid-filled PCF with anomalous dispersion and two zero dispersion points enables a fine control on the spectral correlations.

2. Theoretical description

Degenerate spontaneous four-wave mixing is a third-order non-linear parametric process in which two photons from the pump field E_p with frequency ω_p are annihilated to create a pair of photons: one corresponding to what is called the signal field E_s with frequency ω_s , and the other to the idler field E_i with frequency ω_i . It is a phase-sensitive process, so its efficiency is ruled by the phase-matching condition

$$\Delta k(\omega_s, \omega_i) = 2k(\omega_p) - k(\omega_s) - k(\omega_i) - 2\gamma P = 0, \quad (1)$$

where $k(\omega)$ and γ are the propagation constant and non-linear coefficient of the fiber, respectively, and P is the peak pump power. The frequencies at which the PM condition is fulfilled are called perfect-phase matched frequencies, and are denoted as ω_j^0 , where $j = s, i$.

Following a standard perturbative approach [10], the photon-pair state produced by FWM in an optical fiber can be written as

$$|\psi\rangle \propto \iint d\omega_s d\omega_i f(\omega_s, \omega_i) |\omega_s\rangle |\omega_i\rangle, \quad (2)$$

where $|\omega_s\rangle |\omega_i\rangle$ is a photon-pair state with frequencies ω_s and ω_i , and $f(\omega_s, \omega_i)$ is the joint spectral amplitude (JSA) function, which describes the spectral correlations of the photon-pair state. The JSA function has the form of a convolution integral which can be solved numerically, but some physical insight can be gained by rewriting it in a closed analytical form. This can be done under some approximations.

Assuming the pump envelope function, $\alpha(\omega_s, \omega_i)$, can be modeled as a Gaussian function with linewidth σ , written in terms of the detunings around the perfect phase-matched frequencies, $\Omega_j = \omega_j - \omega_j^0$, as

$$\alpha(\omega_s, \omega_i) = \exp \left[-\frac{(\Omega_s + \Omega_i)^2}{2\sigma^2} \right], \quad (3)$$

and using a first order Taylor expansion of the PM condition around the perfect phase-matched frequencies,

$$\Delta k_{lin}(\omega_s, \omega_i) = \tau_s \Omega_s + \tau_i \Omega_i, \quad (4)$$

the JSA function can be written as the product between the pump envelope function and the phase-matching function, $\phi(\omega_s, \omega_i)$, such that $f(\omega_s, \omega_i) \approx \alpha(\omega_s, \omega_i) \phi(\omega_s, \omega_i)$.

Here, $\tau_j = k_p^{(1)}(\omega_p^0) - k_j^{(1)}(\omega_j^0)$ is the group velocity mismatch between the pump at its central frequency and the signal/idler photon at its perfect-matched frequency, and $k_j^{(1)}(\omega_j^0) = \frac{dk}{d\omega}|_{\omega_j^0}$ is the inverse group velocity. The PM function for a fiber of length L is

$$\phi(\omega_s, \omega_i) = \text{sinc} \left[\frac{L}{2} \Delta k_{lin} \right] \exp \left[i \frac{L}{2} \Delta k_{lin} \right]. \quad (5)$$

The joint spectral intensity (JSI), $|f(\omega_s, \omega_i)|^2$, is an observable and contains all the information about the system, in particular about the spectral factorability and the spectral correlations of the photon pair. When mapped in the $\{\omega_s, \omega_i\}$ space, from the geometry of the JSI it is possible to learn about the amount of information that the knowledge of the idler (signal) photon can provide about the signal (idler) photon, i.e. about the spectral correlations of the photon pair [23]: correlated states form a tilted ellipse, while factorable states can form a circle (symmetric states), or a vertical or horizontal ellipse (asymmetric states). The pump envelope function always has a diagonal orientation, so the shape of the PM function can either compensate or reinforce that behavior. The key factors that influence the shape of the joint-spectral function are the orientation of the PM function with respect to the ω_s axis,

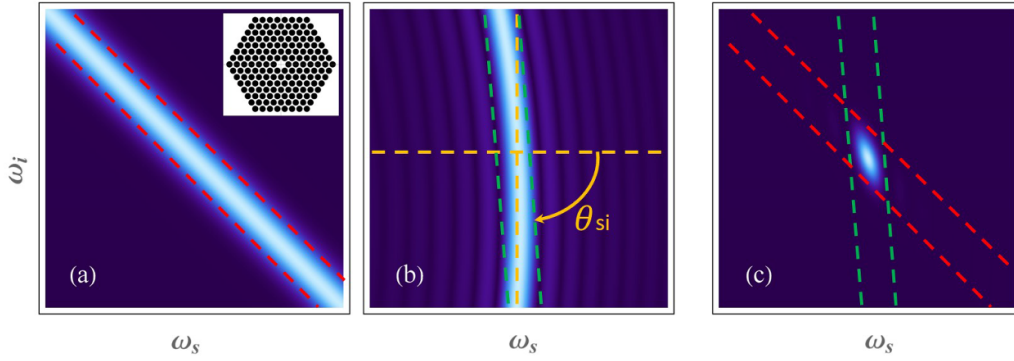


Figure 1. Schematic plots for: (a) pump envelope function $|\alpha(\omega_s, \omega_i)|$, (inset: schematic cross-section of the proposed PCF: white area represents silica, black area represents heavy water), (b) phase-matching function, $|\phi(\omega_s, \omega_i)|$, and its orientation angle θ_{si} , and (c) joint spectral intensity, $|f(\omega_s, \omega_i)|^2$. The orientation angle of the PM function plays an important role in the shape of the JSI.

$\theta_{si} = -\arctan \tau_s / \tau_i$, the pump linewidth $\Delta\omega_p$ and the fiber length L . Figure 1 schematically shows how the JSI is constructed from the pump envelope and phase-matching functions; it also shows the orientation angle θ_{si} and its relevance in the shape of the JSI. The inset of figure 1(a) shows the schematic cross-section of the proposed solid-core PCF: the white area represents silica while the black area represents heavy water.

Practical information about the regime in which a factorable state can be achieved is obtained by approximating the PM function to a Gaussian function ($\text{sinc}(L\Delta k/2) \approx \exp(-(rL\Delta k/2)^2)$, with $r=0.439$). It has been shown [10] that the condition $\tau_s \tau_i \leq 0$ must be fulfilled and that factorable photon-pairs with symmetric spectra can be obtained if the symmetric GVM (SGVM) condition $\tau_s = -\tau_i$ (or $\theta_{si} = \pi/4$) is met. Likewise, asymmetric factorable photon-pairs can be obtained under the asymmetric GVM (AGVM) condition: $\tau_s = 0$ or $\tau_i = 0$ ($\theta_{si} = 0$ or $\theta_{si} = \pi/2$). Thus, in order to obtain a factorable state, the dispersion profile of the fiber needs to be carefully engineered. Photonic crystal fibers with two ZDW exhibit closed-loop PM curves and, in principle, all orientation angles can be achieved. This is the mechanism we propose to achieve tunability of the spectral correlations: controlling θ_{si} with temperature.

3. Results and discussion

The proposed solid-core photonic crystal fiber was designed to have two ZDW and achievable GVM when filled with heavy water and pumped at $\lambda_p = 1064$ nm; its geometrical parameters are: pitch $\Lambda = 1.95 \mu\text{m}$ and hole diameter to pitch ratio $d/\Lambda = 0.97$. The theoretical modeling of its propagation constant, chromatic dispersion and mode field diameter for the fundamental mode was carried out using the full vector method (FVM) reported in [24]. Previous experience [21, 22] indicates that the fabrication of a fiber with such parameters is feasible and that the modeling of the dispersion is reliable up to a few percent values of the parameters.

The wavelength-dependent refractive index of heavy water is included through the Sellmeier coefficients reported in [20],

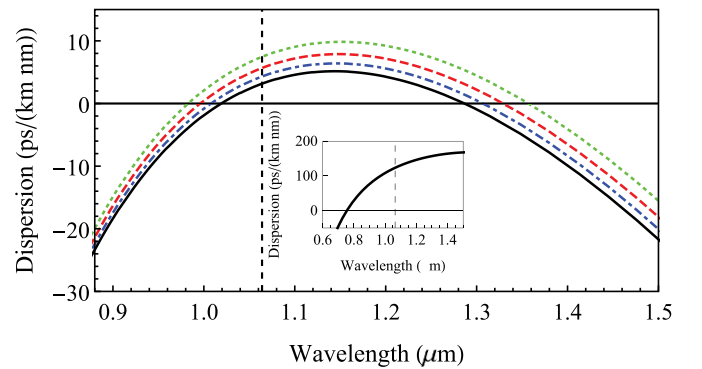


Figure 2. Chromatic dispersion as a function of wavelength calculated for the proposed PCF filled with heavy water at different temperatures: $T = 15^\circ\text{C}$ (solid black), $T = 30^\circ\text{C}$ (dot-dashed blue), $T = 60^\circ\text{C}$ (dashed red) and $T = 100^\circ\text{C}$ (dotted green). The dashed vertical line indicates $\lambda_p = 1064$ nm. Inset: dispersion for the air-filled PCF.

whereas the dominant temperature T effects are incorporated using the heavy water thermo-optic coefficient (TOC), $dn/dT = -6.6 \times 10^{-5} \text{ }^\circ\text{C}^{-1}$ [25], so that the heavy water refractive index, $n(T)$, decreases linearly with T . The contribution of silica to the thermal response of the infiltrated fiber was neglected since silica's TOC, $8.6 \times 10^{-6} \text{ }^\circ\text{C}^{-1}$ [26], is almost one order of magnitude lower than that of heavy water. Both the non-linear refractive index coefficient of water, and its temperature dependence, have been neglected in our simulations, as in previous reported works in which good agreement with experiments was reported [21, 22].

Figure 2 shows the calculated dispersion profiles of the infiltrated PCF for different temperatures. The dispersion curve for the PCF with air is shown as an inset. The air-filled fiber has one ZDW, calculated around $\lambda_{\text{ZDW}} = 755$ nm, while the liquid-filled fiber displays a parabolic dispersion curve with two ZDW, around $\lambda_{\text{ZDW}} = 1010$ nm and $\lambda_{\text{ZDW}} = 1300$ nm at $T = 20^\circ\text{C}$. This dispersion profile opens the possibility to achieve GVM with a pump wavelength at 1064 nm, and with signal and idler wavelengths compatible with available single photon detectors.

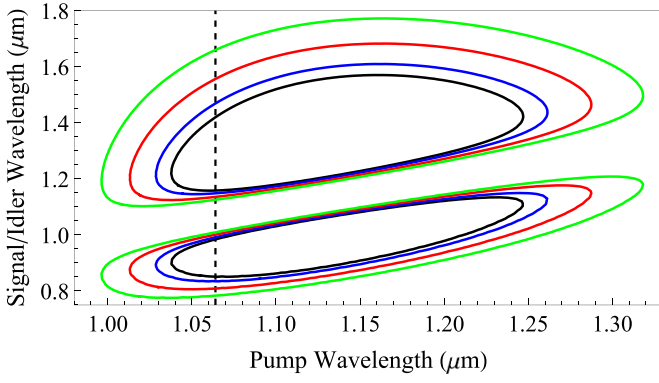


Figure 3. Phase-matching curves for the infiltrated PCF at different temperatures: $T = 15\text{ }^{\circ}\text{C}$ (black), $T = 30\text{ }^{\circ}\text{C}$ (blue), $T = 60\text{ }^{\circ}\text{C}$ (red) and $T = 100\text{ }^{\circ}\text{C}$ (green). The dashed vertical line indicates $\lambda_p = 1064\text{ nm}$.

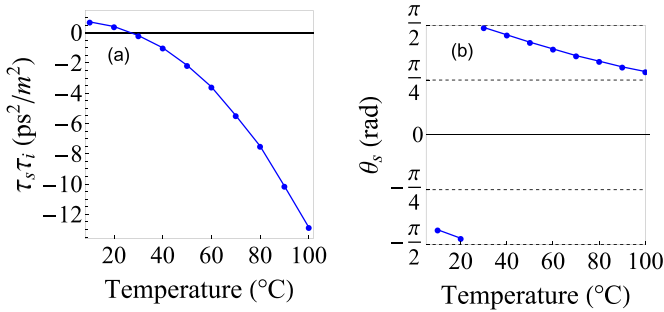


Figure 4. (a) Product $\tau_s \tau_i$ as a function of temperature; (b) orientation of the PM function with temperature. Both calculated for $\lambda_p = 1064\text{ nm}$. The lines are only meant to be a guide for the eyes.

The response of the FWM process in the proposed heavy water-filled PCF was investigated through the phase-matching curves shown in figure 3, considering a peak pump power of $P = 350\text{ W}$. As it is expected, the PM curves have a closed-loop geometry. The signal-idler spectral separation for the external bands increases with increasing temperature, with a predicted spectral tuning from 850 nm to 782 nm for the signal, and from 1420 nm to 1660 nm for the idler in the studied temperature range; both wavelength ranges lay within the detection bands of currently available SPD.

The GVM technique provides a way to achieve high purity. Figure 4(a) shows the product of the group velocity mismatch coefficients, $\tau_s \tau_i$, as a function of temperature for $\lambda_p = 1064\text{ nm}$ for the PCF here proposed; the condition for factorable states, $\tau_s \tau_i \leq 0$, is fulfilled for temperatures around $T = 30\text{ }^{\circ}\text{C}$ and above. Figure 4(b) shows the orientation of the PM function, θ_{si} , with temperature for $\lambda_p = 1064\text{ nm}$. The condition for AGVM, $\theta_{si} = \pi/2$ is met at around $T = 30\text{ }^{\circ}\text{C}$, while $\theta_{si} = 0$ cannot be fulfilled in the studied temperature range. The condition for SGVM is nearly met at $T = 100\text{ }^{\circ}\text{C}$.

Additional factors that determine the factorability are the pump spectral linewidth, $\Delta\lambda_p$, and the fiber length, L . Figure 5 shows results for the JSI in the wavelength space $\{\lambda_s, \lambda_i\}$ for different fiber lengths and temperatures, considering a pump linewidth $\Delta\lambda_p = 2.0\text{ nm}$. It is evident how the JSI shape is

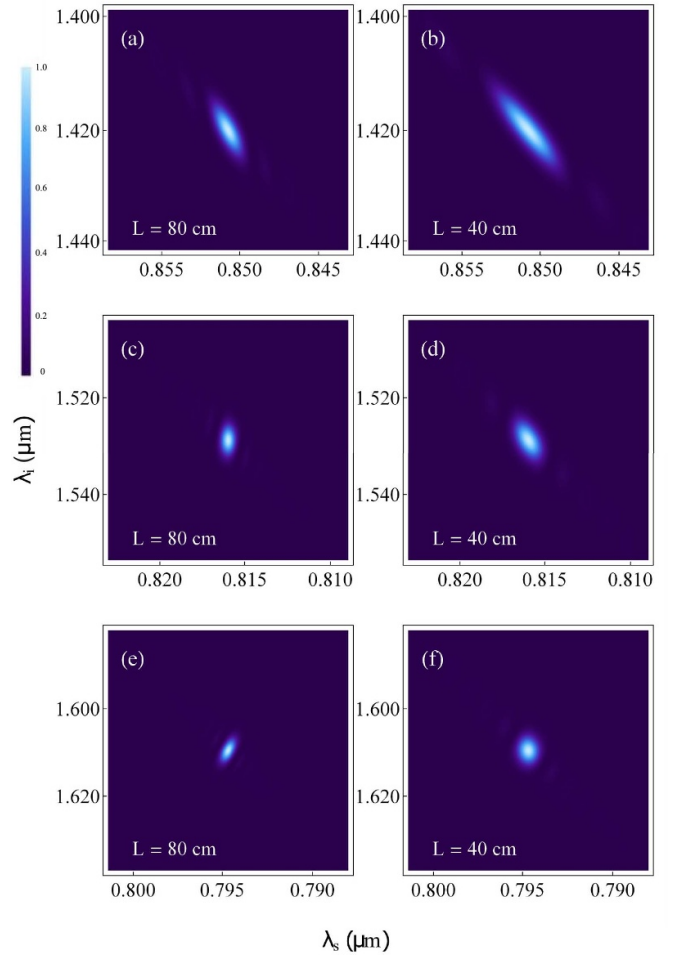


Figure 5. JSI maps for different temperatures and fiber lengths, $\lambda_p = 1064\text{ nm}$ and $\Delta\lambda_p = 2.0\text{ nm}$: (a), (b) $T = 15\text{ }^{\circ}\text{C}$; (c), (d) $T = 50\text{ }^{\circ}\text{C}$; (e), (f) $T = 80\text{ }^{\circ}\text{C}$.

modified by temperature effects, ranging from a tilted ellipse (highly correlated photons) at low temperatures, to a vertical ellipse or even a circle (factorable state) at higher temperatures, all these possibilities for a same fiber length and pump parameters.

The heralded single-photon purity can be obtained through the second-order correlation function $g^{(2)}$ of the signal or idler field. The measurement of the intensity auto-correlations allows the determination of the number of spectral modes in which the signal or idler photon is generated. A beam in a single mode exhibits a thermal distribution and has a value of $g^{(2)} = 2$, whereas light in multiple spectral modes exhibits a Poissonian distribution and the expected value of $g^{(2)} \rightarrow 1$ [27]. Thus, we are interested in the second-order correlation function integrated over time [28],

$$g^{(2)}(t_1, t_2) = \frac{\int dt_1 dt_2 \langle \hat{E}_1^{(-)} \hat{E}_2^{(-)} \hat{E}_1^{(+)} \hat{E}_2^{(+)} \rangle}{\int dt_1 \langle \hat{E}_1^{(-)} \hat{E}_1^{(+)} \rangle \int dt_2 \langle \hat{E}_2^{(-)} \hat{E}_2^{(+)} \rangle}, \quad (6)$$

where $\hat{E}_i = \hat{E}(t_i)$, ($i = 1, 2$).

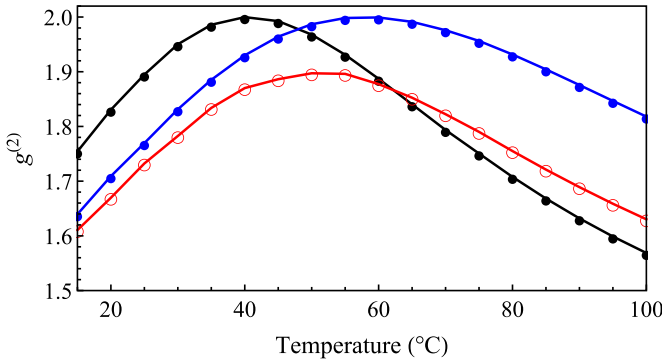


Figure 6. $g^{(2)}$ as a function of temperature for different fiber lengths: $L = 100$ cm (black filled circle) and $L = 60$ cm (blue filled circle), calculated using (7); for comparison, $g^{(2)}$ for $L = 60$ cm (red open circle) calculated numerically without approximation. $\lambda_p = 1064$ nm and $\Delta\lambda_p = 2.0$ nm.

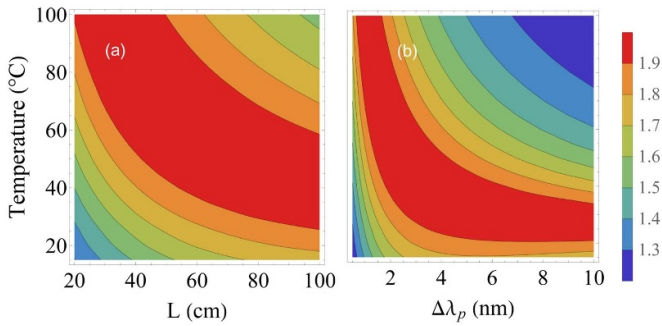


Figure 7. Approximated values of $g^{(2)}$ calculated using (7) as a function of temperature and: (a) fiber length L (with $\Delta\lambda_p = 2.0$ nm), and (b) pump linewidth $\Delta\lambda_p$ (with $L = 60$ cm).

A closed analytical form of (6) can be obtained with the linear approximation of the PM condition (4) and the Gaussian approximation of the PM function [13], such that

$$g^{(2)} = 1 + \frac{1}{\sqrt{1 + \frac{(\tau_s \tau_i (rL\sigma/\sqrt{2})^2 + 1)^2}{(\tau_s - \tau_i)^2 (rL\sigma/\sqrt{2})^2}}} \quad (7)$$

The value of $g^{(2)}$ as a function of temperature for pump wavelength $\lambda_p = 1064$ nm and pump linewidth $\Delta\lambda_p = 2.0$ nm was calculated for fiber lengths $L = 100$ cm and 60 cm using the approximation in (7). One needs to be careful with the values of $g^{(2)}$ that this approximation yields, since experimental conditions differ greatly from it, and the *sinc* function in equation (5) significantly affects the value of $g^{(2)}$. However, this inspection gives useful information about the behavior of $g^{(2)}$ against the different parameters analyzed in this work. For comparison, $g^{(2)}$ was also obtained numerically integrating (6) for $L = 60$ cm; the maximum percentage difference between both results is 10%. Figure 6 shows the results from both the analytical expression (7) and the numerical integration of (6); $g^{(2)}$ increases with temperature until it reaches a turning point and decreases.

Contour maps for the value of $g^{(2)}$ as a function of temperature and fiber length or pump linewidth were calculated

using (7) and are shown in figure 7. These maps are a rich source of information, keeping in mind that an experimental implementation would not produce photons with a $g^{(2)}$ close to 2, which corresponds to the peak values in figure 6 and the red regions in figure 7.

To conclude, we have presented a solid-core photonic crystal fiber design with temperature-controlled dispersion that opens the possibility for dynamic, external tuning of the spectral correlations of a photon-pair state produced by FWM, with no need to change fiber length or pump parameters. It is noteworthy the fact that, after the best configuration for fiber length and pump linewidth is chosen, spectral correlations ranging from highly correlated to pure heralded single photon can be accomplished by only tuning the temperature within a range of a few tens of °C.

Acknowledgments

L V I and J L L would like to acknowledge PRODEP (511-6/18-8876), Universidad de Guanajuato (CIIC-155/2019, CIIC 68/2019) and CONACyT (APN-624). A D, E S and M V A acknowledge Ministerio de Ciencia e Innovación and Fonds Européen de Développement Économique et Régional (FEDER) (PID2019-104276RB-I00), and the Generalitat Valenciana of Spain (PROMETEO/2019/048).

ORCID iDs

Lorena Velázquez-Ibarra  <https://orcid.org/0000-0002-5867-7992>
 Antonio Díez  <https://orcid.org/0000-0003-1045-0411>
 Enrique Silvestre  <https://orcid.org/0000-0002-4092-8597>
 Miguel V Andrés  <https://orcid.org/0000-0003-0103-8644>

References

- [1] Abouraddy A F, Nasr M B, Saleh B E A, Sergienko A V and Teich M C 2002 Quantum-optical coherence tomography with dispersion cancellation *Phys. Rev. A* **65** 053817
- [2] Bennett C H, Brassard G, Crépeau C, Jozsa R, Peres A and Wootters W K 1993 Teleporting an unknown quantum state via dual classical and einstein-podolsky-rosen channels *Phys. Rev. Lett.* **70** 1895–9
- [3] Ekert A K 1991 Quantum cryptography based on bell’s theorem *Phys. Rev. Lett.* **67** 661–3
- [4] Jennewein T, Simon C, Weihs G, Weinfurter H and Zeilinger A 2000 Quantum cryptography with entangled photons *Phys. Rev. Lett.* **84** 1895–9
- [5] Bennett C H and Brassard G 1984 Quantum cryptography: public key distribution and coin tossing *Proc. IEEE Int. Conf. on Computers, Systems and Signal Processing* pp 175–9
- [6] Schiavon M, Vallone G, Ticozzi F and Villoresi P 2016 Heralded single-photon sources for quantum-key-distribution applications *Phys. Rev. A* **93** 012331
- [7] Goldschmidt E A, Eisaman M D, Fan J, Polyakov S V and Migdall A 2008 Spectrally bright and broad fiber-based heralded single-photon source *Phys. Rev. A* **78** 013844

- [8] Yang L, Ma X, Guo X, Cui L and Li X 2011 Characterization of a fiber-based source of heralded single photons *Phys. Rev. A* **83** 053843
- [9] Fulconis J, Alibart O, Wadsworth W J, Russell P St J and Rarity J G 2005 High brightness single mode source of correlated photon pairs using a photonic crystal fiber *Opt. Express* **13** 7572–82
- [10] Garay-Palmett K, McGuinness H J, Offir Cohen J S, Rangel-Rojo L, R, U'Ren A B, Raymer M G, McKinstrie C J, Radi S and Walmsley I A 2007 Photon pair-state preparation with tailored spectral properties by spontaneous four-wave mixing in photonic-crystal fiber *Opt. Express* **15** 14870–86
- [11] Francis-Jones R J A, Hoggarth R A and Mosley P J 2016 All-fiber multiplexed source of high-purity single photons *Optica* **3** 1270–3
- [12] Petrov N L and Fedotov A B and 2019 High-brightness photon pairs and strongly antibunching heralded single photons from a highly nonlinear optical fiber *Opt. Commun.* **450** 304–7
- [13] Cui L, Li X and Zhao N 2012 Minimizing the frequency correlation of photon pairs in photonic crystal fibers *New J. Phys.* **14** 123001
- [14] Pourbeyram H and Mafi A 2018 Photon pair generation with tailored frequency correlations in graded-index multimode fibers *Opt. Lett.* **43** 2018–21
- [15] Fang B, Cohen O, Liscidini M, Sipe J E and Loren V O 2014 Fast and highly resolved capture of the joint spectral density of photon pairs *Optica* **1** 281–4
- [16] Cordier M, Orioux A, Debord B, Gérôme F, Gorse A, Chafer M, Diamanti E, Delaye P, Benabid F and Zaquine I 2019 Active engineering of four-wave mixing spectral correlations in multiband hollow-core fibers *Opt. Express* **27** 9803–14
- [17] Ortiz-Ricardo E, Bertoni-Ocampo C, Ibarra-Borja Z, Ramirez-Alarcon R, Cruz-Delgado D, Cruz-Ramirez H, Garay-Palmett K and U'Ren A B 2017 Spectral tunability of two-photon states generated by spontaneous four-wave mixing: fibre tapering, temperature variation and longitudinal stress *Quantum Sci. Technol.* **2** 034015
- [18] Finger M A, Joly N Y, Russell P St J and Chekhova M V 2017 Characterization and shaping of the time-frequency schmidt mode spectrum of bright twin beams generated in gas-filled hollow-core photonic crystal fibers *Phys. Rev. A* **95** 053814
- [19] Lin Q, Yaman F and Agrawal G P 2007 Photon-pair generation in optical fibers through four-wave mixing: role of Raman scattering and pump polarization *Phys. Rev. A* **75** 023803
- [20] Kedenburg S, Vieweg M, Gissibl T and Giessen H 2012 Linear refractive index and absorption measurements of nonlinear optical liquids in the visible and near-infrared spectral region *Opt. Mat. Express* **2** 1588–1611
- [21] Velázquez-Ibarra L, Díez A, Silvestre E and Andrés M V 2016 Wideband tuning of four-wave mixing in solid-core liquid-filled photonic crystal fibers *Opt. Lett.* **41** 2600–3
- [22] Velázquez-Ibarra L, Díez A, Silvestre E and Andrés M V 2019 Tunable four-wave mixing light source based on photonic crystal fibers with variable chromatic dispersion *J. Lightwave Technol.* **37** 57225726
- [23] Grice W P, U'Ren A B and Walmsley I A 2001 Eliminating frequency and space-time correlations in multiphoton states *Phys. Rev. A* **64** 063815
- [24] Silvestre E, Pinheiro-Ortega T, Andrés P, Miret J J and Ortigosa-Blanch A 2005 Analytical evaluation of chromatic dispersion in photonic crystal fibers *Opt. Lett.* **30** 453–5
- [25] Granville P 1979 Dye lasers *Quantum Electronics, Volume 15 of Methods in Experimental Physics* (New York Academic) p 251–359
- [26] Leviton D B and Frey B J 2008 Temperature-dependent absolute refractive index measurements of synthetic fused silica arXiv:<https://arxiv.org/abs/0805.0091>
- [27] Loudon R 2001 *The Quantum Theory of Light* 3rd edn (Oxford: Oxford University Press)
- [28] Christ A, Laiho K, Eckstein A, Cassemiro K N and Silberhorn C 2011 Probing multimode squeezing with correlation functions *New J. Phys.* **13** 033027